Available online at www.sciencedirect.com

ScienceDirect

Nuclear and Particle Physics Proceedings 258–259 (2015) 51–54

www.elsevier.com/locate/nppp

Jet Production at HERA and Determination of α_s

Artem Baghdasaryan[a,b,*]

[a] DESY (German Electron Synchrotron)
Notkestrasse 85, 22607 Hamburg, Germany
[b] Yerevan Physics Institute
Alikhanian Brothers Street 2, Yerevan, Armenia 0036

Abstract

Inclusive jet, dijet and trijet differential cross sections are measured [1] in neutral current deep-inelastic scattering (DIS) for exchanged boson virtualities $150 < Q^2 < 15000\ GeV^2$ using the H1 detector at HERA. The data were taken in the years 2003 to 2007 and correspond to an integrated luminosity of 351 pb^{-1}. Jet cross sections are obtained using a regularised unfolding procedure. Normalised differential jet cross sections are also measured as the ratio of the jet cross sections to the inclusive neutral current cross sections in the respective Q^2 bins of the jet measurements. The cross sections are used to determine the strong coupling constant $\alpha_s = 0.1165\ (8)_{\rm exp}\ (38)_{\rm pdf,theo}$.
Trijet differential cross sections are measured [2] in neutral current DIS for $125 < Q^2 < 20000\ GeV^2$ using the ZEUS detector at HERA. Good agreement between data and NLO calculations is observed.

Keywords: jet production, normalised to DIS cross sections, regularised unfolding, strong coupling extraction

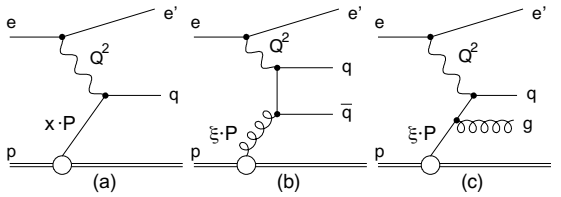

Figure 1: Diagrams of deep-inelastic lepton-proton scattering. (a) Born contribution, (b) boson-gluon fusion, (c) QCD Compton scattering. $\xi = x(1 + M_{12}^2/Q^2)$, where the variables x, M_{jj} and Q^2 denote the Bjorken scaling variable, the invariant mass of the two jets and the negative four-momentum transfer squared, respectively.

1. Introduction

Jet production in neutral current (NC) ep deep-inelastic scattering (DIS) is an important process to study the strong interaction and its theoretical description by Quantum Chromodynamics (QCD). In contrast to inclusive DIS jet production allows for a direct measurement of the strong coupling α_s in the Breit frame of reference [3, 4], where the virtual boson collides head on with a parton from the proton and the Born level contribution to DIS (Fig. 1a) can not generate transverse momentum. Significant transverse momentum P_T in the Breit frame is produced at leading order (LO) in the strong coupling α_s by boson-gluon fusion (Fig. 1b) and the QCD Compton (Fig. 1c) processes.

Double-differential measurements with H1 detector are presented of absolute and normalised inclusive jet, dijet and trijet cross sections in the Breit frame. Two different jet algorithms, k_T [5] and $anti-k_T$ [6], are explored. The cross sections are measured as a function of Q^2 , the jet transverse momentum $P_{T,jet}$ for inclusive jet and the average transverse momentum for dijet and trijet. The ratios of the number of jets to the number of inclusive NC DIS events in the respective bins of Q^2, referred to as normalised multijet cross sections, are also measured. In comparison to absolute jet cross sections these measurements profit from a significant reduction of the systematic experimental uncertainties. The measurements are compared to perturbative QCD predictions at NLO, corrected for hadronisation effects, and are used for strong coupling α_s extraction.

The production of trijets in NC DIS has been measured with the ZEUS detector using the integrated luminosity of 295 pb^{-1}. The measurements was performing in the kinematical region $125 < Q^2 < 20000\ GeV^2$ and inelasticity $0.2 < y < 0.6$. Jet are reconstructed in the Breit frame using inclusive k_T-algorithm.

*Speaker
Email address: artem.baghdasaryan@desy.de (Artem Baghdasaryan)

http://dx.doi.org/10.1016/j.nuclphysbps.2015.01.012
2405-6014/© 2015 Elsevier B.V. All rights reserved.

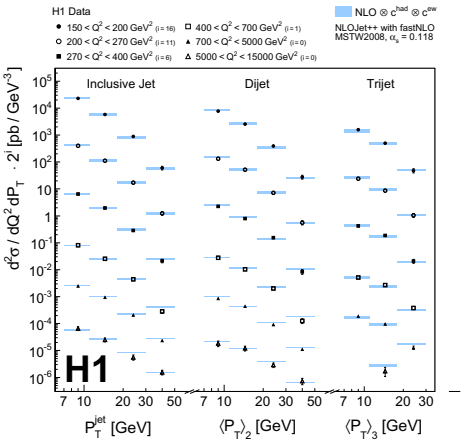

Figure 2: Double-differential cross sections for jet production in DIS as a function of Q^2 and $P_{T,jet}$. The inner and outer error bars indicate the statistical uncertainties and the statistical and systematic uncertainties added in quadrature. The NLO QCD predictions, corrected for hadronisation and electroweak effects, together with their uncertainties are shown by the shaded band. The cross sections for individual Q^2 bins are multiplied by a factor of 10i for better readability.

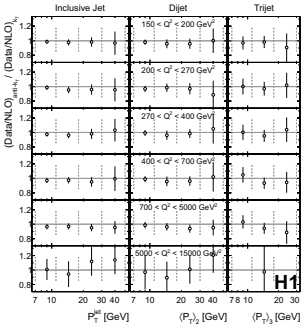

Figure 3: Comparison of cross section measured using the k_T algorithm and the $anti-k_T$ algorithm. Shown are the double-differential double-ratios of $anti-k_T$ jet cross sections to NLO predictions divided by the ratio of k_T jet cross sections to their NLO predictions.

2. Normalised to DIS jet cross section measurement and α_s extraction

Jet cross sections are measured as a function of Q^2 and $P_{T,jet}$ for inclusive jet and average $< P_{T,jet} >$ for di- and trijet production. Measured cross sections are presented in Fig. 2. Measurements using $anti-k_T$-algorithm are very close to the measurements using k_T-algorithm. This is demonstrated in Fig. 3, where the double-ratio of $anti-k_T$ jet cross sections to NLO predictions to k_T jet cross sections to NLO predictions is presented. The error bars correspond to the $anti-k_T$ experimental uncertainties. The simultaneous unfolding of the NC DIS and the jet measurements allows the determination of jet cross sections normalised to the NC DIS cross

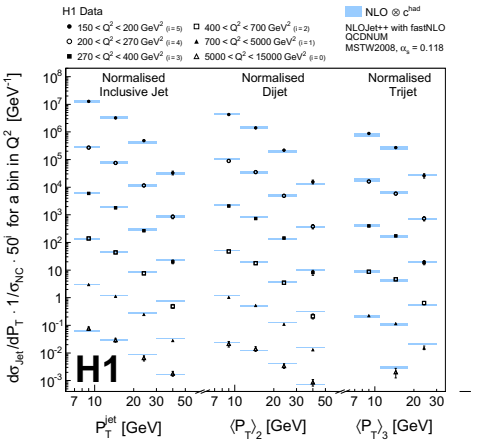

Figure 4: Normalised double-differential cross sections for jet production in DIS as a function of Q^2 and $P_{T,jet}$.

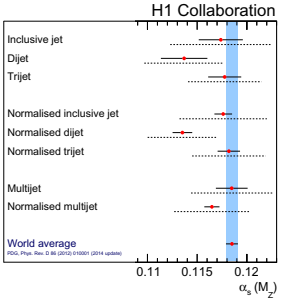

Figure 5: Comparison of $\alpha_s(M_Z)$ extracted from different jet cross section measurements, separately and simultaneously, to the world average value of $\alpha_s(M_Z)$. The full line indicates the experimental uncertainty and the dashed line the theoretical uncertainty. The band indicates the uncertainty of the world average value of $\alpha_s(M_Z)$.

sections. Normalised jet cross sections are defined as the ratio of the double-differential absolute jet cross sections to the NC DIS cross sections in the respective Q^2-bin. The phase space for the normalised inclusive-, di- and trijet cross sections is identical to the one of the corresponding absolute jet cross sections. The covariance matrix of the statistical uncertainties is determined taking into account the statistical correlations between the NC DIS and the jet measurements. The systematic experimental uncertainties are correlated between the NC DIS and the jet measurements, therefore correlated systematic uncertainties are canceled for normalised cross sections. Measured normalised cross sections are presented in Fig. 4. The measured jet cross sections are used to determine the value of the strong coupling constant $\alpha_s(M_Z)$, in the framework of perturbative QCD. The value of the strong coupling constant α_s is determined in an iterative χ^2-minimisation procedure

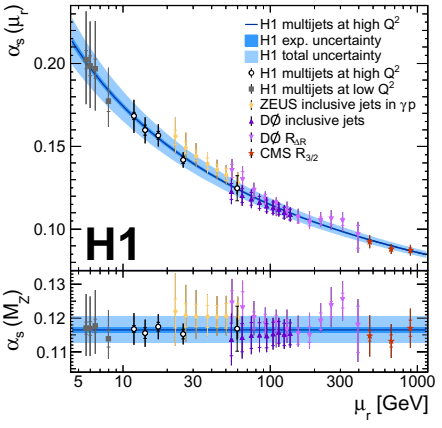

Figure 6: Comparison of $\alpha_s(M_Z)$ extracted from different jet cross section measurements, separately and simultaneously, to the world average value of $\alpha_s(M_Z)$. The full line indicates the experimental uncertainty and the dashed line the theoretical uncertainty. The band indicates the uncertainty of the world average value of $\alpha_s(M_Z)$.

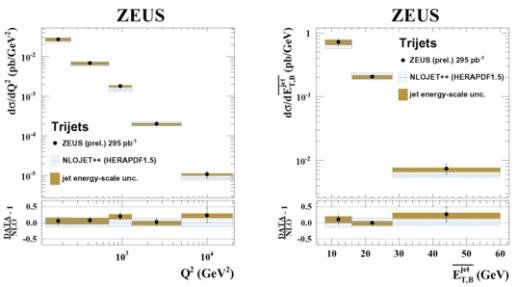

Figure 7: The measured differential trijet production cross section vs. Q^2 (left) and vs. $E_{T,jet,B}$ (right). The inner error bars represent the statistical uncertainty. The outer error bars show the statistical and systematical uncertainties, not associated with the uncertainty on the absolute energy scale of the jet. The shaded bands display the uncertainties due to the absolute energy scale of the jets. The hatched bands display the estimated total theoretical uncertainty. The lower part of the figure schows the relative difference between data and theory prediction.

using NLO calculations, corrected for hadronisation and electroweak effects. For the α_s-fit, the evolution of $\alpha_s(\mu_r)$ is performed, using the renormalisation group equation in two-loop precision with five massless flavours. The strong coupling constant is determined from each of the jet measurements, as a function of Q^2 and $P_{T,jet}$, as well as from the three absolute and three normalised jet cross sections simultaneously. The statistical correlations are taken into account. The α_s-values obtained from measurements using the k_T jet algorithm are compared to those using the $anti-k_T$ jet algorithm with the corresponding NLO calculations. The best experimental precision on α_s is obtained from a fit to normalised multijet cross sections, yielding: $\alpha_s(M_Z)|_{k_T} = 0.1165\ (8)_{exp}\ (5)_{PDF}\ (7)_{PDFset}\ (3)_{PDF(\alpha_s)}\ (8)_{had}\ (36)_{\mu_r}\ (5)_{\mu_f} = 0.1165\ (8)_{exp}\ (38)_{pdf,theo}$. This value of α_s obtained using the k_T algorithm is fully consistent with the α_s-value found for jets using the $anti-k_T$ algorithm. The experimental precision benefits from the reduced jet energy scale uncertainty, reduced uncertainties of normalised jet cross sections, the large phase space of the inclusive jet data and the increased sensitivity to $\alpha_s(M_Z)$ of the trijet data. The uncertainties on $\alpha_s(M_Z)$ are dominated by theory uncertainties from missing higher orders and allow a determination of $\alpha_s(M_Z)$ with a precision of 3.4% only, while an experimental precision of 0.7% is reached. The determined values of α_s (Fig 5) are compatible with the world average [7] value of $\alpha_s(M_Z) = 0.1185\ (6)$ within the experimental and particularly the theoretical uncertainties. The running of $\alpha_s(\mu_r)$ is determined from five fits using the normalised multijet cross sections, each based

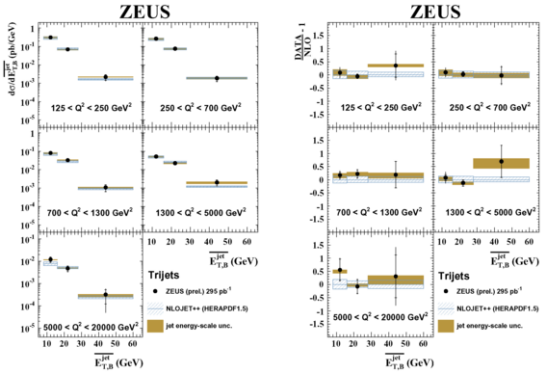

Figure 8: The measured differential trijet production cross section for regions of Q^2: absolute values (left), relative difference between data and NLO prediction (right)

on a set of measurements with comparable values of the renormalisation scale μ_r. The values of $\alpha_s(M_Z)$ and $\alpha_s(\mu_r)$ obtained from the k_T-jets are displayed in Fig 6 together with results from other jet data [8–12]. Within the small experimental uncertainties the values of $\alpha_s(M_Z)$ of the present analysis are consistent and independent of μ_r. Good agreement is found with H1 data [8] at low scales and other jet data [9–12] at high scales. The prediction for the running of μ_r using $\alpha_s(M_Z) = 0.1165\ (8)_{\rm exp}\ (38)_{\rm pdf,theo}$, as extracted from the normalised multijet cross sections, is also shown in Fig 6, together with its experimental and total uncertainty. The prediction is in good agreement with the measured values of $\alpha_s(\mu_r)$.

3. Trijet production cross section

The trijet cross sections in NC ep DIS have been measured with the ZEUS detector at HERA. The measurements was performed in the kinematic region $125 < Q^2 < 20000\ GeV^2$ and $0.2 < y < 0.6$. Jets were reconstructed in the Breit frame with the inclusive k_T algorithm. The jet were required to lie in the kinematic region $E_{T,jet,B} > 8\ GeV$ and $-1. < \eta_{jet,lab} < 2.5$, where $E_{T,jet,B}$ is the jet transverse momentum in the Breit frame and $\eta_{jet,lab}$ - the jet pseudorapidity in the laboratory frame. In Fig. 7 left and Fig. 7 right differential cross sections vs. Q^2 and vs. $E_{T,jet,B}$ for trijet production are shown . The data are compared to NLO prediction [13] with the HERAPDF1.5 set [14]. Renormalisation and factorisation scales are equal to $\mu_r^2 = Q^2 + < E_{T,jet,B} >^2$ and $\mu_f^2 = Q^2$ correspondingly. In Fig. 8 (left) are shown double differential cross sections vs. $E_{T,jet,B}$ in Q^2 bins and in Fig. 8 (right) - relative difference between data and NLO theory prediction. The theoretical predictions describe the data within uncertainties.

4. Conclusions

Measurements of inclusive jet, dijet and trijet cross sections in the Breit frame in deep-inelastic electron-proton scattering with the H1 detector at HERA in the kinematical range $150 < Q^2 < 15000\ GeV^2$ and $0.2 < y < 0.7$ are presented. The measurements consist of absolute jet cross sections as well as jet cross sections normalised to the neutral current DIS cross sections. Jets are determined using the k_T and the $anti-k_T$ jet algorithm. The jet cross section measurements are performed using a regularised unfolding procedure to correct the neutral current DIS, the inclusive jet, the dijet and the trijet measurements simultaneously for detector effects. Theoretical QCD calculations at NLO, corrected for hadronisation and electroweak effects, provide a good description of the measured double-differential jet cross sections as a function of the exchanged boson virtuality Q^2, the jet transverse momentum $P_{T,jet}$, the mean transverse momentum in case of dijets and trijets. In general, the precision of the data is considerably better than that of the NLO calculations. The measurements are used to extract values for the strong coupling constant $\alpha_s(M_Z)$. The best experimental precision of 0.7% is obtained when using the normalised multijet cross sections. Strong coupling constant $\alpha_s(M_Z)$ from the normalised jet samples using the k_T jet algorithm yields: $\alpha_s(M_Z)|_{k_T} = 0.1165\ (8)_{exp}\ (5)_{PDF}\ (7)_{PDFset}\ (3)_{PDF(\alpha_s)}\ (8)_{had}\ (36)_{\mu_r}\ (5)_{\mu_f} = 0.1165\ (8)_{exp}\ (38)_{pdf,theo}$. A very similar result is obtained when using the $anti-k_T$ jet algorithm. The running of α_{μ_r}, determined from the normalised multijet cross sections, is shown to be consistent with the expectation from the renormalisation group equation and with values of $\alpha_s(\mu_r)$ from other jet measurements.

Trijet differential cross sections are measured with ZEUS detector at HERA in neutral current DIS in the kinematical range $125 < Q^2 < 20000\ GeV^2$ and $0.2 < y < 0.7$. Good agreement between data and NLO calculations is observed.

References

[1] H1 Collab., DESY-14-089, [arxiv:1406.4709].
[2] ZEUS Collab., ZEUS-prel-14-008.
[3] R. Feynman, *Photon - Hadron Interactions*. Benjamin, New York, 1972.
[4] K. Streng, T. Walsh, and P. Zerwas, Z. Phys. **C 2** (1979) 237.
[5] S. Ellis and D. Soper, Phys. Rev. D **48** (1993) 3160, [hep-ph/9305266].
[6] M. Cacciari, G. P. Salam, and G. Soyez, JHEP **0804** (2008) 063, [arXiv:0802.1189].
[7] S. Bethke, Nucl. Phys. Proc. Suppl. **234** (2013) 229, [arXiv:1210.0325].
[8] H1 Collaboration, Eur. Phys. J.C **67** (2010) 1, [arXiv:0911.5678].
[9] ZEUS Collaboration, Nucl. Phys. B **864** (2012) 1, [arXiv:1205.6153].
[10] D0 Collaboration, Phys. Rev. D **80** (2009) 111107, [arXiv:0911.2710].
[11] D0 Collaboration, Phys. Lett. B **718** (2012) 56, [arXiv:1207.4957].
[12] CMS Collaboration, Eur. Phys. J.C **73** (2013) 2604, [arXiv:1304.7498].
[13] Z. Nagy and Z. Trocsanyi, Phys. Rev. Lett. **87** (2001) 082001, [hep-ph/0104315].
[14] H1 and ZEUS Collaborations, Preliminary result, H1prelim-10-142, ZEUS-prel-10-018, 2010.